Paper: ASAT-17-027-ET

17th International Conference on
AEROSPACE SCIENCES & AVIATION TECHNOLOGY,
ASAT - 17 – April 11 - 13, 2017, E-Mail: asat@mtc.edu.eg
Military Technical College, Kobry Elkobbah, Cairo, Egypt
Tel: +(202) 24025292 – 24036138, Fax: +(202) 22621908

Characterization of 3D Printed Stainless Steel SS316L Powders Joined by TIG-, Plasma- and Laser Welding

M. Harraz[*], N. El-Mahallawy[†], K. Abd Elghany[‡], M. Schleser[§], H. Palkowski[**], A. Klingner[††]

Abstract: Additive manufacturing or 3D printing is becoming more and more common in industry fabrication especially for spare parts which cannot be found easily on the local market and for tailor made parts. For large parts and due to its size limitations it is sometimes required to join 3D printed parts with other 3D printed parts or conventionally produced parts. In this work 3D printed flat plates 4mm thick were prepared by direct laser sintering of SS316L powders. Mechanical properties and microstructure were investigated. Elongation and maximum tensile stress of 3D printed flat plates are with 1.3% and 704MPa close to the values 2% and 1241MPa of cold-rolled SS316 parts. The 3D printed flat plates were joined by welding using TIG welding, Plasma welding and Laser welding. The welded joints were tested for their mechanical properties and microstructure. For the used welding conditions, the fracture occurred outside the weld zone. The maximum stress of the welded parts is 65-80% of 3D printed flat plates. The elongation of the welded parts is above 3%.

Keywords: 3D printing, additive manufacturing, welding, SLM, SS316L

1. Introduction

3D printing (or additive manufacturing) is a form of rapid prototyping technology which allows for the fabrication of 2 or 3 dimensional products via a layer by layer materials build-up method. Its relevance as a mainstream tool for series production has grown significantly over the past 10 years [1]. While 3D printing techniques remain less competitive to conventional (subtractive) manufacturing methods (such as milling, grinding, cutting, casting, rolling, etc.) in terms of high volume production, it brings along a profound advantage in terms of the possibility of easily fabricating complex geometry components and the customization of components to be deployed to highly specialized engineering systems. Such a technical merit brings 3D printing technologies to an industrial foreground where its application alongside other manufacturing techniques is being explored. There are five most widely applied forms of 3D printing techniques namely Fused Deposition Modeling (FDM), Stereolithography (SLA), Inkjet Printing, Laminated Object Manufacturing (LOM), Selective Laser Melting (SLM) and Selective Laser Sintering (SLS). Each of these methods is unique in

[*] Engineering Materials, Faculty of Engineering Materials Science, The German University in Cairo – GUC, Main Entrance Al Tagamoa Al Khames, New Cairo City, 13411, Egypt, mohamed.harraz@guc.edu.eg .
[†] Engineering Materials, Faculty of Engineering Materials Science, The German University in Cairo – GUC, Main Entrance Al Tagamoa Al Khames, New Cairo City, 13411, Egypt, nahed.el-mahallawy@guc.edu.eg .
[‡] Laser and Additive Manufacturing Lab, Central Metallurgical Research and Development Institute (CMRDI), El-Tebeen, Helwan, 11422, Cairo, Egypt, khalidghany@gmail.com
[§] FH Aachen, University of Applied Sciences, D-52064 Aachen Germany, Schleser@fh-aachen.de
[**] Werkstoffumformung im IMET, Institut fuer Metallurgie, TU Clausthal, Germany, D-38678 Clausthal-Zellerfeld, heinz.palkowski@tu-clausthal.de
[††] Department of Physics, Basic Science, The German University in Cairo – GUC, Main Entrance Al Tagamoa Al Khames, New Cairo City, 13411, Egypt, anke.klingner@guc.edu.eg

the sense that the kinds and forms of materials used as feedstock as well as the approach to materials build-up into a three-dimensional form are different. For metal processing the SLM and SLS methods are applied. These methods use a laser source to fuse together metallic powder particles in a layer by layer fashion until a dense part is built-up. By altering the beam parameters (power, flux etc.) and scan strategies (rate, direction etc.), new and unusual, even non-equilibrium microstructures can be produced; including controlled microstructural architectures which ideally extend the contemporary materials science and engineering paradigm relating structure-properties-processing-performance [2-4]. For 3D printed parts the importance of testing on essentially every part cannot be over stressed especially since 3D Printing technology has still not been fully technically assessed and characterized [5]. To understand the technical capabilities of 3D printed parts, the systematic examination and testing of parts need to be conducted. The main tests are carried out using tensile testing, hardness and microhardness testing and others depending on the application of the product. Among the properties measured are the modulus of elasticity, yield point, ultimate tensile strength and ductility. These can be obtained from the tensile test applied on samples with standard shape and dimensions. Hardness and microhardness tests give an indication about the resistance to surface scratching and wearing of the material [6]. Furthermore, the product size and dimensions of 3D printing are restricted by the size of the platform of each 3D printing machine (typically a surface area no more than 300 mm x 500m, and a height of about 600 mm), which is not large enough for big parts. Therefore, in order to produce large components, a solution could be to subdivide the component into several parts then to join these parts together. The joining of metallic parts is a key process in technical practice. Welding, fasteners (nuts and bolts) as well as application of adhesive bonds are the main joining methods applied in industry. These methods account for a huge portion of investment in engineering construction. For instance welding is an essential manufacturing step in the automotive and aerospace industries. It provides both joining and repair value in these industries. Very few information is available in the literature on how to use joining techniques on 3D printed parts and the kind of mechanical properties and microstructure induced at the joint zones. Comparison of welded wrought and SLM parts have been studied by Casalino et al. [7] and Järvinen [8].

The primary goal of this study is to see the influence of the welding process on the weld properties of steel samples prepared by SLM. Microstructural examination as well as the mechanical test on the welded parts will be correlated to the 3D printing conditions thus allowing for the determination of the optimal conditions for producing good weld joints of the studied materials.

2. Sample Preparation

The preparation of the samples consists of several steps such as 3D printing, welding and preparation for characterization which are explained in the following. A summary of the samples is given in Table 2.

3D Printing

3D printing of the samples was performed at a rapid prototyping machine “M3 linear concept laser” located at Central Metallurgical Research and Development Institute (CMRDI). The specimens were produced from SS316L powders. The SS316L powder was purchased from Powder manufacturer in China and the chemical composition was determined as shown in the Table 1 below. The apparent density was between 3.5g/cm^3 and 5g/cm^3. The particle size is determined by 400 mesh which translates into a layer size of 50 micrometers. The 3D process uses laser for the micro-melting and welding of fine powder particles in stacked layers until the complete part is built. The process is based on sintering powder as squares 5mmx5mm randomly on the surface. This process depends strongly on the process parameters to get high

strength and crack free products. Here, the parameters applied are: laser power 200W, scanning speed 800 mm/min, line overlap 30%, focus diameter 0.15 mm, scanning islands 5mm x 5mm, and layer thickness 50 micrometer. The specimens were built with an orientation angle of 45 degrees relative to the base.

Table 1 Chemical composition of SS316L powder.

Cr	Ni	Mo	C	Mn	Cu	P	S	Si	N	Fe
18.00	14.00	2.50	0.03	2.00	0.50	0.0025	0.010	0.75	0.10	Rest

Welding

The samples are welded by TIG, Plasma welding and laser welding as shown in Fig. 1. The welding processes TIG and Plasma welding are done on two phases. The first stage (pilot arc) is usually done with higher energy than the normal welding arc as to initiate the molten zone in the weld to proceed. This pilot arc usually takes fraction of second and is in the range of 100-110 Amp for TIG welding and then goes down to about 50-60 Amp. For plasma welding the pilot arc is about 70 Amp and then goes down to 45 Amp during the constant state welding and for the second paths. The welding for the high sample thickness is done by 2 welding paths (root and cap). The nozzle had a size Ø2.4 mm. The welding wire was GGS 1.4576, EN ISO 14343-A:W 19 12 3 Nb Si with chemical composition of C:0,06 Si:0,80 Mn:1,40 Cr:19,00 Ni:12,00 Mo:2,60 Nb:0,7 and diameter of 1.6mm. Yield strength and elongation are 450MPa and 30%, respectively. Laser welding was done with CO2-Laser RS6000 with handling from Balliu, welding speed: 1300 mm/min, power: 1100 W (35% activation with small opening, Gaussian power distribution, shielding and working gas: He 20 l/min, optic: off-axis -parabolic mirror, focal length: 150 mm. The process conditions for welding with its specific welding parameters are summarized in Table 2.

Fig. 1. Welding regions produced by TIG welding (left), Plasma welding (middle) and Laser welding (right).

Table 2 Welding parameters.

Weld	Process	Filler	Current [A]
16-598	TIG	GGS 1.4576	100
16-597, 16-599	TIG	GGS 1.4576	105
Weld 1	TIG	GGS 1.4576	110
Weld 4, 5	Plasma	GGS 1.4576	60
Weld 3	Plasma	GGS 1.4576	70
Weld 2	Plasma	GGS 1.4576	80
16-700	Laser	GGS 1.4576	1100 Watt

Microstructure investigation

In order to examine the microstructure of the specimen, it had to be prepared for observation under the optical microscope. The welded samples and broken samples from the tensile test were mounted in Bakelite through compression mounting. The mounted samples were wet

ground using different grades of silicon carbide grinding paper from P60 through P180, P360, P360, P800, and P1000 to finally P1200. This process was followed by polishing using polycrystalline diamond suspension gel.
An etchant constituting of equal parts water, nitric acid and hydrochloric acid was used to etch the polished sample. Microstructure was observed before and after etching using an optical microscope.

Tensile Test

For tensile testing dogbone shapes according to ASTME8/E8M-13a specimen specification were prepared. They have a total length 60mm, neck length 20mm, total width 12 mm, neck width 6mm and thickness 4mm. The samples were not produced directly at dogbone shape during 3D printing because welding has to be done on straight sections. Therefore, the samples received by 3D printing were cut to dogbone shape for tensile testing after welding. Straight sections have been cut with diamond cutter and remaining parts were removed with machining. The tensile strength of the samples were measured by Zwick Roell machine Z100. The specimens were fixed with wedge screw holders. A macro extensometer was used. The test speed was 5mm/min.

Hardness Measurements

The Vickers hardness test equipment (Zwick / Rowell) was set to a loading of 15 kg and 20 kg to get HV15 and HV20.

Corrosion Measurements

Open Circuit Potential (OCP) and Potential Cyclic Voltammetry (PCV) experiments were conducted with Voltalab 10 PGZ 100 (www.radiometer - analytical.com, Figure 2) to determine the electrochemical corrosion rate (ECR). The corroding solution was NaCl 3.5%. Reference electrode was SCE and auxiliary electrode Platinum.

3. Results and Discussion

SLS has been used as an additive manufacturing method to produce specimens from stainless steel powder. These specimen have been welding by three different welding processes, namely TIG welding, Plasma welding and Laser welding. The welding regions for the three processes are shown in Fig. 1. At first the microstructure of the samples is discussed. Then hardness profiles and tensile test results are given. The observation of the macrostructure indicates that the welding regions look differently depending on the welding process as shown in Figures 2-4. The overviews reveal a size of the welding region with the heat effected zone (HAZ) of more than 5mm for TIG welding and Plasma welding, whereas the size is less than 1mm for laser welding. The HAZ is 1-2mm wide for TIG welding and Plasma welding, but only 0.1mm for laser welding. These results are expected as the laser welding is known to have a deep penetration and very small HAZ. The base material shows the structure of the 3D printing process with the lines of laser melting. The 3D printed steel contained some oxides and cavities due to the melting of powders. After etching the typical austenitic stainless steel microstructure was observed. The microstructure of the weld cross-sections show more dense and pore-free weld region compared to the base material, denoting a successful weld. There is some excess material above the weld zone for all welding processes due to deposited filler material. The HAZ has less porosity than the base material and the building structures of 3D printing are less pronounced than in the base material due to the transformation by the induced heat.
In TIG welded sample weld 1 dentritic structures are visible in the weld zone. In the welding zone small particles of 1 micrometer diameter appear. Two phases are visible which seem to come from powder and filler.

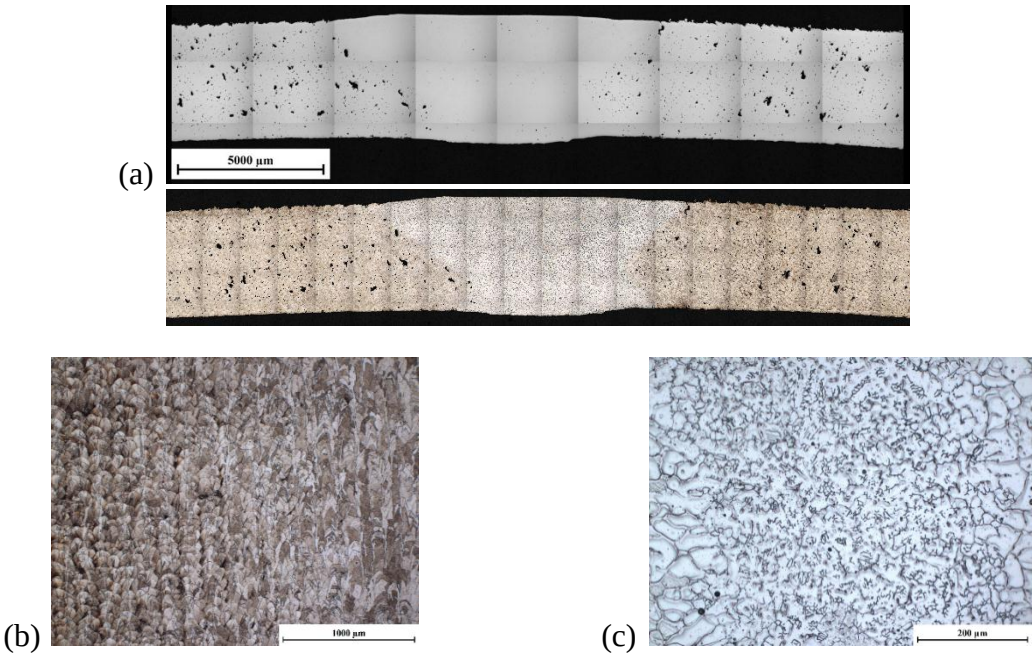

Fig. 2. Microstructure of TIG welding. (a) Overview of weld 1 with 5000µm scale bar before and after etching, (b) base material and HAZ of 16-597 with 1000µm scale bar, (c) weld region of 16-597 with 200µm scale bar.

For Plasma welded sample weld 2, no dentritic structures have been seen in the welded zone indicating less energy input than for weld 1. Plasma welded weld 3 shows more fine pores in the base material than weld 2. There is a dentritic structure in the weld zone. The structure of the two phases is finer than in weld 1. For Plasma welded sample weld 4 the weld region is framed by a thin line. This thin line consists of very fine structures of gray phase. Some dentrites are visible but not in the whole welding zone.

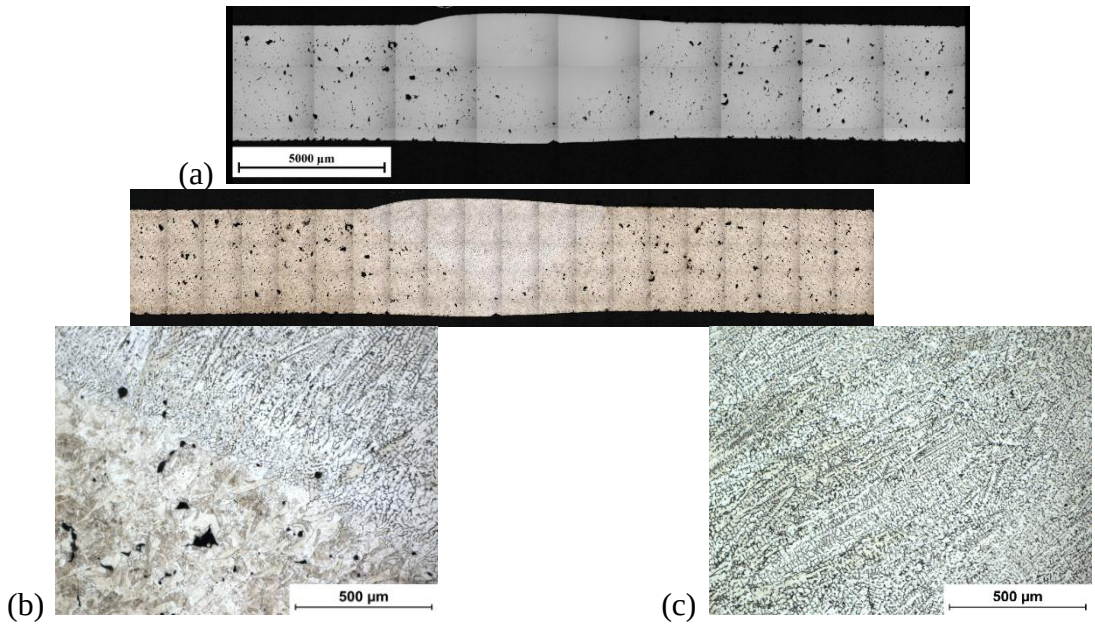

Fig. 3. Microstructure of Plasma welding. (a) Overview of weld 5 before and after etching with 5000µm scale bar, (b) HAZ and weld region od weld 3 with 500µm scale bar, (c) weld region with 500µm scale bar.

For laser welded sample a clear welding centerline is visible. There is some excess material outside the weld. The weld zone is about 0.3mm wide 1.2mm wide at the top. in the bottom and In summary, the welded region shows dendritic structures and no porosity.

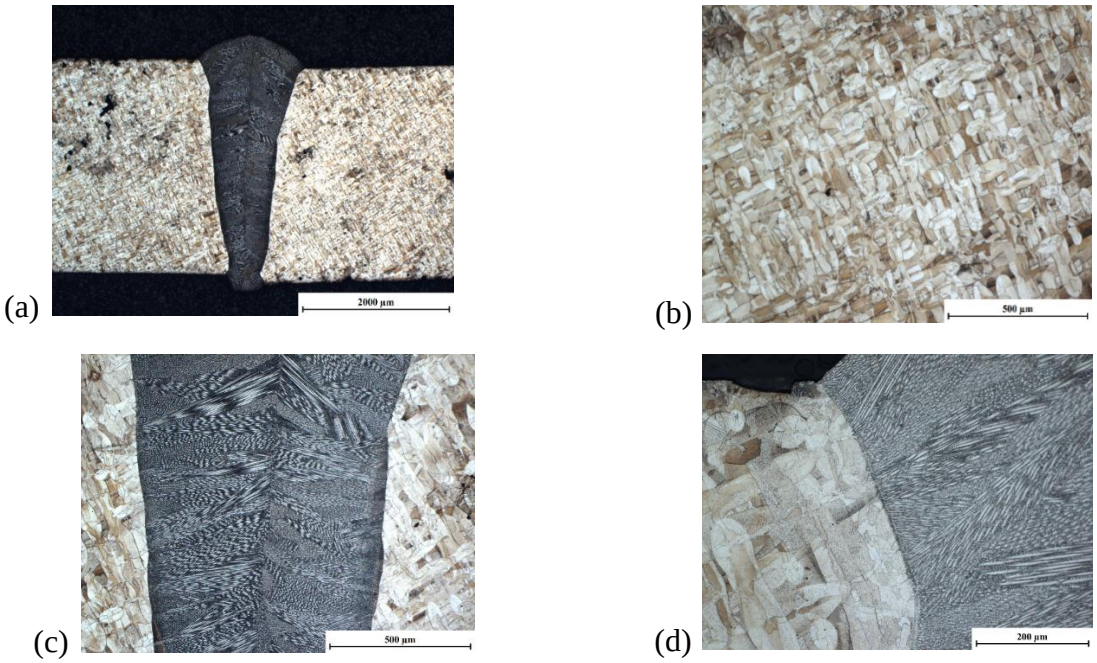

Fig. 4. Microstructure of laser welding. (a) Overview with 2000µm scale bar, (b) base material with 500µm scale bar, (c) weld region with 500µm scale bar and (d) weld and HAZ with 200µm scale bar.

Mechanical properties were tested by hardness profiles and tensile tests. Points of hardness measurements with the indenter are visible in Fig. 5. Hardness decreases in the weld region for all welding conditions. For TIG welding and Plasma welding the hardness decreased from 230-250 in the base material to 160-190 in the weld region. The hardness in the HAZ is between these values. For laser welding, the hardness is about 230 in the base material and 225 in the weld region. This hardness decrease is less pronounced than for Plasma welding and TIG welding. That the hardness of the weld zone is below the hardness of the SLM produced base material was also observed by Casalino et al. [7]. This could result from the difference in chemical composition of the filler with respect to the base material and to the difference in cooling rates.

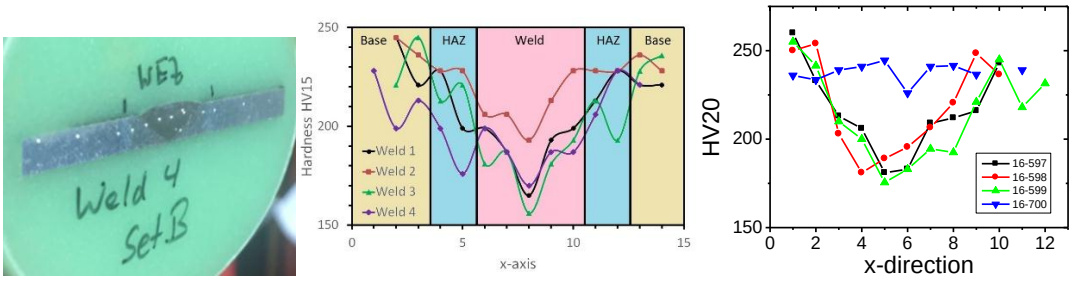

Fig. 5. Embedded welded sample with hardness indentations and hardness profiles of the samples.

During tensile tests fracture occurred in the base material as shown in Fig. 6. The results of tensile tests such as maximum stress and elongation are summarized in Table 3. The maximum stress of all samples is almost in between hot rolled and cold rolled values found in

literature. The highest values of maximum stress have been found for the base material and the laser welded sample. The laser welding showed with 9% a higher elongation than the base material. The TIG welded sample had an intermediate maximum stress of 539MPa and elongation of 4.5%. The Plasma welded samples had maximum stress in the range of 453MPa – 563MPa and elongation of 3.8% - 8.3%. The maximum stress increased with welding current for Plasma welded samples.

a) Weld 1 b) Weld 2

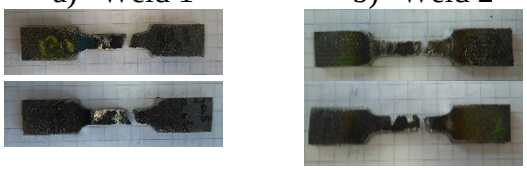

Fig. 6. Fractured samples after tensile tests.

Table 3 Results of tensile tests.

Sample	Process	Max. Stress [N/mm^2]	Elongation [%]
SS hot rolled [8]	hot rolled	485	40
SS cold rolled [9]	cold rolled	1241	2
Base material	3D printed	704	1.3
Weld 1	TIG	539	4.5
Weld 2	Plasma	563	6.4
Weld 3	Plasma	534	4.5
Weld 4	Plasma	453	8.3
Weld 5	Plasma	459	3.8
16-700	Laser	700	9

Corrosion test has been done in the weld region and compared to corrosion outside the weld region for weld 1, TIG. The corrosion in the weld/HAZ zone is with 0.6 µm/yr smaller than the corrosion of the base material with about 2 µm/yr. The method of welding effects greatly the macrostructure, the microstructure, the extent of heat effected zone and the mechanical properties. The laser welding shows highest tensile strength, ductility and hardness.

4. Conclusions

Stainless steel samples were successfully prepared by 3D Direct Laser melting of powders. The samples welded by TIG, Plasma and Laser welding. The weld zone was free of pores in all welds. The strength of the Laser weld reached 700 MPa with 9% elongation while Plasma and TIG welds resulted in lower strength and ductility with a strength of 459 to 563 MPa with elongation of 3.8 to 6.4% for Plasma welds and 539 MPa with 4.5% elongation for TIG weld. The corrosion rate was lower in the TIG weld with 0.6µm/yr than in the base metal with 2µm/yr. For effective joining of small parts with thicknesses below 4mm, a laser power of 1100 Watt has proven to achieve a complete welding penetration in one path and the welding process was reproducible. In case of Plasma and TIG welding the process needs to be automated or semi-automated to achieve reproducible results. It would be useful to carry out more mechanical testing to characterize additive manufactured materials and their welds further. Fatigue tests and Residual stresses measurements are planned in the future.

Acknowledgement

This research has been conduct under the DAAD-BMBF project "Optimization of 3D printed metallic parts for laser welding". We would like to thank for this support.

5. References

[1] Roland Berger Strategy Consultants "Additive manufacturing, A game changer for the manufacturing industry?", Munich, November 2013.

[2] L.N. Carter, C. Martin, P.J. Withers, M.M. Attallah "The influence of the laser scan strategy on grain structure and cracking behaviour in SLM powder-bed fabricated nickel superalloy" *Journal of Alloys and Compounds* 615, 2014, pp. 338–347.

[3] S.M. Kelly, S.L. Kamper "Microstructural evolution in laser-deposited multilayer Ti–6Al–4V builds: Part 1. Microstructural characterization", *Metall. Mater. Trans. A (Phys. Metall. Mater. Sci.)* 35 A, 2004, pp. 1861–1867.

[4] L.E. Murr, S.M. Gaytan, D.A Ramirez, E. Martinez, J. Hernandez, K.N. Amato, P.W. Shindo, F.R.Medina, R.B.Wicker, "Metal Fabrication by Additive Manufacturing Using Laser and Electron Beam Melting Technologies (Review)" *Journal of Materials Science and Technology* 28, 2012, pp. 1-14.

[5] A. Gebhardt, *Rapid prototyping*, 1st ed., Hanser publisher, Munich, 2003.

[6] W. Callister, *Materials science and engineering. An introduction*, 7th ed., Willey publisher, 2007.

[7] Casalino, G., Campanelli, S. L., Ludovico, A. D. "Laser-arc hybrid welding of wrought to selective laser molten stainless steel." *The International Journal of Advanced Manufacturing Technology*, 68, 2013, pp. 209-216.

[8] "Stainless Steel - Grade 316L - Properties, Fabrication and Applications (UNS S31603)", http://www.azom.com/article.aspx?ArticleID=2382, accessed 15.01.2017.

[9] SS 316L TECHNICAL DATA SHEET, Hamilton Precision Metals, 1780 Rohrerstown Road, Lancaster, PA 17602, SS-316L.pdf, accessed 10.05.2015.

[10] Selcuk, C., Bond, S., Woollin, P. "Joining processes for powder metallurgy parts: a review." *Powder Metallurgy*, *53*(1), 2010, pp. 7-11.

[11] Järvinen, J. P. "Welding of additively manufactured stainless steel parts: Comparative study between sheet metal and selective laser melted parts", Master's Thesis, 2014.